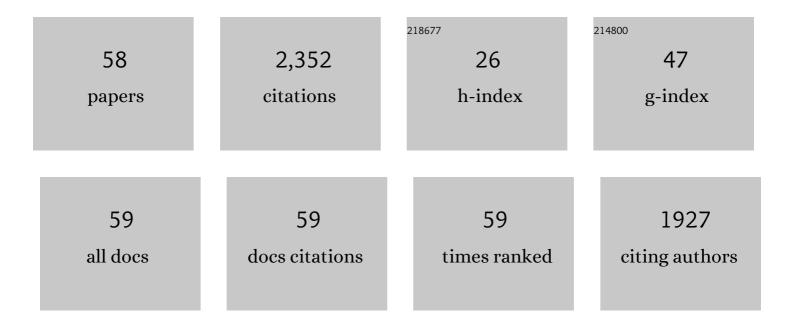
## Jianping Long

List of Publications by Year in descending order

Source: https://exaly.com/author-pdf/1074809/publications.pdf Version: 2024-02-01



#	Article	IF	CITATIONS
1	Adjusting the d-band center of metallic sites in NiFe-based Bimetal-organic frameworks via tensile strain to achieve High-performance oxygen electrode catalysts for Lithium-oxygen batteries. Journal of Colloid and Interface Science, 2022, 607, 1215-1225.	9.4	20
2	Synergy of cobalt vacancies and iron doping in cobalt selenide to promote oxygen electrode reactions in lithium-oxygen batteries. Journal of Colloid and Interface Science, 2022, 612, 171-180.	9.4	11
3	A multifunctional protective layer with biomimetic ionic channel suppressing dendrite and side reactions on zinc metal anodes. Journal of Colloid and Interface Science, 2022, 613, 136-145.	9.4	8
4	Promoted redox chemistry of high sulfur content cathode via endowing fast Li-ion diffusion. Ionics, 2022, 28, 1473-1481.	2.4	0
5	Airflow Synergistic Needleless Electrospinning of Instant Noodleâ€like Curly Nanofibrous Membranes for Highâ€Efficiency Air Filtration. Small, 2022, 18, e2107250.	10.0	28
6	Interlayer material technology of manganese phosphate toward and beyond electrochemical pseudocapacitance over energy storage application. Journal of Materials Science and Technology, 2021, 71, 109-128.	10.7	31
7	Modulating electronic structure of honeycomb-like Ni2P/Ni12P5 heterostructure with phosphorus vacancies for highly efficient lithium-oxygen batteries. Chemical Engineering Journal, 2021, 413, 127404.	12.7	39
8	Boosting pseudocapacitive energy storage performance via both phosphorus vacancy defect and charge injection technique over the CoP electrode. Journal of Alloys and Compounds, 2021, 864, 158106.	5.5	22
9	Modulating in-plane electron density of molybdenum diselenide via spontaneously atomic-scale palladium doping enables high performance lithium oxygen batteries. Journal of Alloys and Compounds, 2021, 855, 157484.	5.5	5
10	An artificial hybrid interphase for an ultrahigh-rate and practical lithium metal anode. Energy and Environmental Science, 2021, 14, 4115-4124.	30.8	376
11	Tuning the Unsaturated Coordination Center of Electrocatalysts toward High-Performance Lithium–Oxygen Batteries. ACS Sustainable Chemistry and Engineering, 2021, 9, 7499-7507.	6.7	6
12	Active site synergy of the mixed-phase cobalt diselenides with slight lattice distortion for highly reversible and stable lithium oxygen batteries. Journal of Materials Science and Technology, 2021, 92, 159-170.	10.7	1
13	Interface-engineered metallic 1T-MoS2 nanosheet array induced via palladium doping enabling catalysis enhancement for lithium–oxygen battery. Chemical Engineering Journal, 2020, 382, 122854.	12.7	52
14	Tuning oxygen non-stoichiometric surface via defect engineering to promote the catalysis activity of Co3O4 in Li-O2 batteries. Chemical Engineering Journal, 2020, 381, 122678.	12.7	68
15	Configuration of gradient-porous ultrathin FeCo <sub>2</sub> S <sub>4</sub> nanosheets vertically aligned on Ni foam as a noncarbonaceous freestanding oxygen electrode for lithium–oxygen batteries. Nanoscale, 2020, 12, 1864-1874.	5.6	22
16	Optimizing Redox Reactions in Aprotic Lithium–Sulfur Batteries. Advanced Energy Materials, 2020, 10, 2002180.	19.5	112
17	Anionic vacancy-dependent activity of the CoSe <sub>2</sub> with a tunable interfacial electronic structure on the N-doped carbon cloth for advanced Li–O <sub>2</sub> batteries. Journal of Materials Chemistry A, 2020, 8, 16636-16648.	10.3	31
18	Promoting the Electrocatalytic Activity of Ti <sub>3</sub> C <sub>2</sub> T <sub>x</sub> MXene by Modulating CO <sub>2</sub> Adsorption through Oxygen Vacancies for Highâ€Performance Lithiumâ€Carbon Dioxide Batteries. ChemElectroChem, 2020, 7, 4922-4930.	3.4	10

JIANPING LONG

#	Article	IF	CITATIONS
19	Tuning the electronic band structure of Mott–Schottky heterojunctions modified with surface sulfur vacancy achieves an oxygen electrode with high catalytic activity for lithium–oxygen batteries. Journal of Materials Chemistry A, 2020, 8, 11337-11345.	10.3	38
20	Rationalizing the Effect of Oxygen Vacancy on Oxygen Electrocatalysis in Li–O <sub>2</sub> Battery. Small, 2020, 16, e2001812.	10.0	81
21	Excellent electrolyte-electrode interface stability enabled by inhibition of anion mobility in hybrid gel polymer electrolyte based Li–O2 batteries. Journal of Membrane Science, 2020, 604, 118051.	8.2	19
22	Invigorating the Catalytic Activity of Cobalt Selenide via Structural Phase Transition Engineering for Lithium–Oxygen Batteries. ACS Sustainable Chemistry and Engineering, 2020, 8, 5018-5027.	6.7	16
23	Interfacial electronic structure design of MXene-based electrocatalyst via vacancy modulation for lithium-oxygen battery. Carbon, 2020, 166, 273-283.	10.3	11
24	Interface engineering induced selenide lattice distortion boosting catalytic activity of heterogeneous CoSe2@NiSe2 for lithium-oxygen battery. Chemical Engineering Journal, 2020, 393, 124592.	12.7	84
25	Heterostructured NiS <sub>2</sub> /ZnIn <sub>2</sub> S <sub>4</sub> Realizing Toroid-like Li <sub>2</sub> O <sub>2</sub> Deposition in Lithium–Oxygen Batteries with Low-Donor-Number Solvents. ACS Nano, 2020, 14, 3490-3499.	14.6	113
26	A 3D free-standing Co doped Ni <sub>2</sub> P nanowire oxygen electrode for stable and long-life lithium–oxygen batteries. Nanoscale, 2020, 12, 6785-6794.	5.6	30
27	Phosphorus vacancies enriched Ni2P nanosheets as efficient electrocatalyst for high-performance Li–O2 batteries. Electrochimica Acta, 2020, 337, 135795.	5.2	39
28	Multifunctional Selenium Vacancy Coupling with Interface Engineering Enables High-Stability Li–O <sub>2</sub> Battery. ACS Sustainable Chemistry and Engineering, 2020, 8, 6667-6674.	6.7	22
29	Defect regulation of heterogeneous nickel-based oxides via interfacial engineering for long-life lithium-oxygen batteries. Electrochimica Acta, 2019, 321, 134716.	5.2	16
30	Heteroatom-Induced Electronic Structure Modulation of Vertically Oriented Oxygen Vacancy-Rich NiFe Layered Double Oxide Nanoflakes To Boost Bifunctional Catalytic Activity in Li–O <sub>2</sub> Battery. ACS Applied Materials & Interfaces, 2019, 11, 29868-29878.	8.0	38
31	Morphology regulation of Li2O2 by flower-like ZnCo2S4 enabling high performance Li-O2 battery. Journal of Power Sources, 2019, 441, 227168.	7.8	49
32	3D porous network gel polymer electrolyte with high transference number for dendrite-free Li O2 batteries. Solid State Ionics, 2019, 343, 115088.	2.7	8
33	Design strategies toward catalytic materials and cathode structures for emerging Li–CO <sub>2</sub> batteries. Journal of Materials Chemistry A, 2019, 7, 21605-21633.	10.3	75
34	Cobalt encapsulated within porous MOF-derived nitrogen-doped carbon as an efficient bifunctional electrocatalyst for aprotic lithium-oxygen battery. Journal of Alloys and Compounds, 2019, 810, 151877.	5.5	20
35	Dendrite-Free Solid-State Li–O <sub>2</sub> Batteries Enabled by Organic–Inorganic Interaction Reinforced Gel Polymer Electrolyte. ACS Sustainable Chemistry and Engineering, 2019, 7, 17362-17371.	6.7	19
36	Three-dimensional CoNi2S4 nanorod arrays anchored on carbon textiles as an integrated cathode for high-rate and long-life Lithiumâ ``Oxygen battery. Electrochimica Acta, 2019, 301, 69-79.	5.2	34

JIANPING LONG

#	Article	IF	CITATIONS
37	Two-dimensional spinel CuCo2S4 nanosheets as high efficiency cathode catalyst for lithium-oxygen batteries. Journal of Alloys and Compounds, 2019, 798, 560-567.	5.5	21
38	Improved Cyclability of Lithium–Oxygen Batteries by Synergistic Catalytic Effects of Two-Dimensional MoS <sub>2</sub> Nanosheets Anchored on Hollow Carbon Spheres. ACS Sustainable Chemistry and Engineering, 2019, 7, 6929-6938.	6.7	31
39	Understanding the Reaction Chemistry during Charging in Aprotic Lithium–Oxygen Batteries: Existing Problems and Solutions. Advanced Materials, 2019, 31, e1804587.	21.0	254
40	In Situ Fabricating Oxygen Vacancy-Rich TiO <sub>2</sub> Nanoparticles via Utilizing Thermodynamically Metastable Ti Atoms on Ti <sub>3</sub> C <sub>2</sub> Tx MXene Nanosheet Surface To Boost Electrocatalytic Activity for High-Performance Li–O <sub>2</sub> Batteries. ACS Applied Materials & Interfaces, 2019, 11, 46696-46704.	8.0	77
41	Highly reversible Li-O2 battery induced by modulating local electronic structure via synergistic interfacial interaction between ruthenium nanoparticles and hierarchically porous carbon. Nano Energy, 2019, 57, 166-175.	16.0	73
42	Free-Standing Three-Dimensional CuCo <sub>2</sub> S <sub>4</sub> Nanosheet Array with High Catalytic Activity as an Efficient Oxygen Electrode for Lithium–Oxygen Batteries. ACS Applied Materials & Interfaces, 2019, 11, 3834-3842.	8.0	75
43	Componentâ€Interaction Reinforced Quasiâ€Solid Electrolyte with Multifunctionality for Flexible Li–O <sub>2</sub> Battery with Superior Safety under Extreme Conditions. Small, 2019, 15, e1804701.	10.0	38
44	NiCo <sub>2</sub> S <sub>4</sub> Nanorod Arrays Supported on Carbon Textile as a Freeâ€Standing Electrode for Stable and Longâ€Life Lithiumâ€Oxygen Batteries. ChemElectroChem, 2019, 6, 349-358.	3.4	15
45	3D Array of Bi <sub>2</sub> S <sub>3</sub> Nanorods Supported on Ni Foam as a Highly Efficient Integrated Oxygen Electrode for the Lithiumâ€Oxygen Battery. Particle and Particle Systems Characterization, 2018, 35, 1700433.	2.3	30
46	Honeycomb-like Ni3S2 supported on Ni foam as high performance free-standing cathode for lithium oxygen batteries. Electrochimica Acta, 2018, 290, 657-665.	5.2	41
47	Three-Dimensional Interconnected Network Architecture with Homogeneously Dispersed Carbon Nanotubes and Layered MoS <sub>2</sub> as a Highly Efficient Cathode Catalyst for Lithium–Oxygen Battery. ACS Applied Materials & Interfaces, 2018, 10, 34077-34086.	8.0	72
48	Threeâ€Dimensional Flowerâ€Like MoS <sub>2</sub> @Carbon Nanotube Composites with Interconnected Porous Networks and High Catalytic Activity as Cathode for Lithiumâ€Oxygen Batteries. ChemElectroChem, 2018, 5, 2816-2824.	3.4	23
49	Luminescence enhancement of (Sr <sub>1–<i>x</i></sub> M <sub><i>x</i></sub> ) <sub>2</sub> SiO <sub>4</sub> :Eu <sup>2</sup> <sup>+phosphors with M (Ca<sup>2</sup><sup>+</sup>/Zn<sup>2</sup><sup>+</sup>) partial substitution for white lightâ€emitting diodes. Luminescence. 2017. 32, 119-124.</sup>	up չ 2.9	7
50	Sol–gel synthesis and luminescence property of Sr <sub>4</sub> Al <sub>2</sub> O <sub>7</sub> :Re3 <sup>+</sup> ,R <sup>+</sup> (ReÂ=ÂEu and Dy; RÂ=ÂLi, Na	a)2.Tg ETQq	1010 0 rgBT /(
51	Synthesis and photoluminescence of Eu <sup>3+</sup> /Dy <sup>3+</sup> -doped CaGdAlO <sub>4</sub> phosphors for white light emitting diodes. Integrated Ferroelectrics, 2017, 179, 148-158.	0.7	3
52	Preparation and modification of polythiophene-organic montmorillonite composite. Polymer Composites, 2016, 37, 2503-2510.	4.6	0
53	Al2O3/TiO2 core/shell powder derived by novel sol–gel routes. Journal of Sol-Gel Science and Technology, 2015, 75, 475-480.	2.4	3
54	Theoretical Investigation of the Newly Noncentrosymmetric Superconductor SrAuSi3 via First Principles. Journal of Superconductivity and Novel Magnetism, 2015, 28, 3235-3241.	1.8	8

JIANPING LONG

#	Article	IF	CITATIONS
55	Effect of replacement of Ca by Zn on the structure and optical property of CaTiO <sub>3</sub> :Eu <sup>3+</sup> red phosphor prepared by solâ€gel method. Luminescence, 2015, 30, 533-537.	2.9	15
56	Luminescence Enhancement of ZnS:Cu Nanocrystals by Zinc Sulfide Coating with Core/Shell Structure. Integrated Ferroelectrics, 2014, 154, 110-119.	0.7	3
57	First-principles calculations of structural phase transition and elastic properties of BeTe under high pressure. Philosophical Magazine Letters, 2014, 94, 103-111.	1.2	5
58	Electrochemical Kinetics of Layered Manganese Phosphate via Interfacial Polypyrrole Chemical Binding. ChemElectroChem, 0, , .	3.4	3